alcohols, carboxylic acids, and acetone. These all show the systematic effects mentioned above. In particular, the linear correlation line between the calculated and experimental acidities has a slope close to 1.2 for all of the calculations.

Because of these systematic errors, lower level ab initio calculations of the sort considered here cannot by themselves give reliable predictions for the acidity. Typical calculated values can deviate from the experimental ones by 0.3 eV and, for different levels of calculation for the same compound, may range over as much as 0.6 eV. However, the correlation coefficients for the linear correlation between experiment and theory are very close to unity. Therefore, the calculated acidities fall very close to the regression lines, and these lines can be used together with calculated numbers to give predicted experimental values close to the true ones. Even though the calculated acidities for a given compound range over 0.6 eV, the values of acidity estimated from these theoretical results and the linear correlations agree with one another within 0.14 eV (3 kcal/mol). These linear correlations can, therefore, be used with the theoretical acidities to make predictions of experimental acidities that are probably within 0.13 eV (3 kcal/mol) of the correct values.

Acknowledgment. This work was supported in part by the National Science Foundation and the Norwegian Council for Scientific and Industrial Research. We are indebted to John Bartmess for providing us with his estimates of the acidities of allyl and isopropenyl alcohol and to Thomas Hellman Morton for a suggestion that led ultimately to this work.

Registry No. Fluoroacetic acid, 144-49-0; fluoroacetate anion, 513-62-2; formic acid, 64-18-6; formate anion, 71-47-6; acetic acid, 64-19-7; acetate anion, 71-50-1; cyclopentadiene, 542-92-7; cyclopentadiene anion, 12127-83-2; 2,2-difluoroethanol, 359-13-7; 2,2-difluoroethanol anion, 104745-47-3; acetone, 67-64-1; acetone anion, 24262-31-5; isopropyl alcohol, 67-63-0; isopropyl alcohol anion, 15520-32-8; ethanol, 64-17-5; ethanol anion, 16331-64-9; methanol, 67-56-1; methanol anion, 3315-60-4; ethene, 74-85-1; ethene anion, 25012-81-1; methane, 74-82-8; methane anion, 15194-58-8; ethane, 74-84-0; ethane anion, 25013-41-6; allyl alcohol, 107-18-6; allyl alcohol anion, 71695-00-6; isopropenyl alcohol, 29456-04-0.

Supplementary Material Available: Tables of optimized geometries and total energies for all of the neutral molecules and their anions (4 pages). Ordering information is given on any current masthead page.

Valency Correlation Diagrams

Prabha Siddarth and M. S. Gopinathan*

Contribution from the Department of Chemistry, Indian Institute of Technology, Madras 600 036, India. *Received April 27, 1987*

Abstract: It is shown that the recently proposed molecular orbital (MO) valency serves as a quantitative ordinate for the Walsh-type correlation diagrams. The essential requirements for a molecular orbital quantity to be a successful ordinate for such correlation diagrams are formulated. Universal correlation diagrams are drawn with MO valency as ordinate for AH_2, AH_3, HAB, and AB_2 classes of molecules and shown to be remarkably similar to the original Walsh diagrams. With the notable exception of core and lone pair orbitals, MO eigenvalues also lead to acceptable correlation diagrams. The question whether the sum of the ordinate quantities leads to the correct bond angle for a given molecule is also examined. It is shown that MO valency predicts the bond angles well whereas the MO eigenvalue often fails in this respect. A simple valency method is proposed to predict bond angles of electronically excited or ionized states of a given molecule by using just its ground-state wave function. This method is shown to be capable of predicting bond angles for excited and ionized states remarkably well.

I. Introduction

Walsh diagrams[1,2] are plots of certain "molecular orbital energies" as a function of some geometry parameter, usually a bond angle. These diagrams have been useful in predicting the geometry of the ground, excited, or ionized states of molecules merely from the number of valence electrons. However, such predictions are only qualitative since Walsh did not precisely define the ordinate "molecular orbital energy" and the Walsh diagrams were based on qualitative arguments regarding atomic overlaps and their relation to molecular orbital (MO) binding energies. This fact has prompted numerous investigators to search for a molecular orbital quantity in the SCF theory that could be used as the ordinate. These attempts have been described in a review by Buenker and Peyerimhoff.[3] Quantities such as MO eigenvalues[4] and their variants[5-7] and MO forces[8] have been tried, but these attempts have been only partially successful. We have recently introduced the idea of a valency for each molecular orbital[9] and have shown that MO valency as the ordinate reproduces the Walsh-type diagrams quite accurately for a few molecules.

In this paper, we first set down the essential properties that a MO quantity should have to qualify as an ordinate for the qualitative Walsh diagrams (Section II). We then examine how well MO valency as well as the usual ordinate, MO eigenvalue, satisfy these criteria (Section III). The quantitative predictions of the equilibrium bond angles for the ground state of molecules by both mo valency and mo eigenvalue are discussed in Sec. IV. In Sec. V, a simple method, which utilizes only the ground state molecular orbitals, is proposed and demonstrated to be remarkably successful for the prediction of bond angles of excited states.

II. Criteria for the Walsh Ordinate

Walsh diagrams are meant to be used only for qualitative predictions of the shape of molecules. The prediction of the exact geometry of a given molecule is not intended. However, there have been some studies in the literature[3,4,10] to see if the sum of the ordinates, normally the eigenvalues, gives the same equilibrium bond angle as does the total energy. While it is desirable to have this property for certain purposes, as will be discussed later, it is not an essential requirement for a Walsh ordinate.

The essential criteria for a MO quantity to serve as a Walsh ordinate may be formulated as follows:

(1) Walsh, A. D. *J. Chem. Soc.* **1953**, (a) 2260, (b) 2266, (c) 2288, (d) 2296, (e) 2301, (f) 2306, (g) 2321.
(2) Mulliken, R. S. *Rev. Mod. Phys.* **1942**, *14*, 204.
(3) Buenker, R. J.; Peyerimhoff, S. D. *Chem. Rev.* **1974**, *74*, 127.
(4) Peyerimhoff, S. D.; Buenker, R. J.; Allen, L. C. *J. Chem. Phys.* **1966**, *45*, 734.
(5) Coulson, C. A.; Neilson, A. H. *Discuss. Faraday Soc.* **1963**, *35*, 71, 217.
(6) Stenkamp, L. Z.; Davidson, E. R. *Theor. Chim. Acta* **1973**, *30*, 283.
(7) Mehrotra, P. K.; Hoffmann, R. *Theor. Chim. Acta* **1978**, *48*, 301.
(8) Coulson, C. A.; Deb, B. M. *Int. J. Quantum Chem.* **1971**, *5*, 411.
(9) Gopinathan, M. S.; Siddarth, P.; Ravimohan, C. *Theor. Chim. Acta* **1986**, *70*, 303.
(10) Allen, L. C.; Russell, J. D. *J. Chem. Phys.* **1967**, *46*, 1029.

0002-7863/88/1510-0096$01.50/0

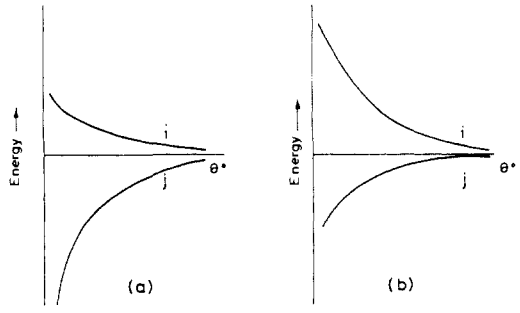

Figure 1. Sketch of two types a and b of variation of MO energies with angle. If both types occur for a given (i,j) pair in a class of compounds, no Walsh diagram can be drawn for this class of compounds.

(1) The sign of the slope of the ordinate with respect to bond angle should be the same for a given MO in all compounds in a particular class. This means, for example, that if $3a_1$ favors a bent structure in a given AH_2 molecule, it should do so in all other AH_2 molecules.

(2) The relative magnitude of the variation of the ordinate with bond angle for a pair of MOs should be the same for a given class of compounds. This condition requires that if the magnitude of the variation in $3a_1$, for example, is greater than that of $1b_2$ for a given AH_2 molecule, it should remain so for all the other molecules of AH_2 type. That this condition is necessary for the qualitative prediction of shape may be easily seen from the schematic sketch in Figure 1. Though the sign of the slope of each MO remains the same in both parts a and b in Figure 1, the relative magnitudes are altered. Thus Figure 1a would predict a bent structure while Figure 1b would predict a linear shape for a molecule where only these two MOs are occupied. It is also easy to see that this condition need only be satisfied by pairs of MOs whose slopes are opposite in sign, since variation in the relative magnitude of slopes of MOs with the same sign will not affect qualitative shape predictions.

(3) For the core and lone pair orbitals, the ordinate should not vary with bond angle. Walsh considered these MOs as not involved in bonding and therefore independent of bond angle. Hence if molecular shape is to be predicted merely from the number of valence electrons, it is essential to satisfy this criterion.

III. MO Valency and Eigenvalue as the Walsh Ordinate

In this section, we examine in detail how well the molecular orbital valency and canonical orbital eigenvalue perform as Walsh ordinate in the sense of satisfying the above three criteria. We have studied in all 52 molecules (see Table I) by STO-3G wave functions.[11] The bond lengths were kept constant at the optimized values corresponding to the theoretical equilibrium.

Valency of an atom in a molecule has been previously defined[12-14] as

$$V_A = \sum_{a}^{A} \sum_{B \neq A} \sum_{b}^{B} P_{ab}^2 \qquad (1)$$

and the total valency of the molecule has been given[9] as

$$V_M = \tfrac{1}{2} \sum_{A} V_A \qquad (2)$$

Table I. Bond Angles Obtained by Molecular Valency (V_M), Sum of Valence Orbital Eigenvalues (E'_{VAL}), Total Energy (E_T), and Experimental Values

molecule	bond angle by V_M	E'_{VAL}[a]	E_T	exptl[b]
AH_2				
1. LiH_2	180	180	180	
2. BH_2^+	180	180	180	
3. BH_2	130	120	122	131
4. BH_2^-	180	<90	98	102[c]
5. CH_2^+	135	120	136	131[c]
6. CH_2 ($^1A_1$)	100	90	100	102
7. CH_2^-	93	<90	96	99[c]
8. NH_2^+	95	<90	112	115[c]
9. NH_2	100	<90	103	103
10. NH_2^-	115	<90	103	104
11. H_2O^+	105	<40	109	112
12. H_2O	100	50	100	104
13. FH_2^+	95	<90	112	118[c]
14. H_2S	92	<70	92	92
AH_3				
1. BH_3	120	120	120	
2. BH_3^-	120	80	120	
3. CH_3^+	120	120	120	
4. CH_3	120	120	120	
5. CH_3^-	102	92	112	105[c]
6. NH_3^+	120	95	120	
7. NH_3	104	<40	104	107
8. H_3O^+	95	<70	115	110[c]
9. SiH_3^-	95	98	96	101[c]
10. PH_3	85	90	94	93[c]
11. SH_3^+	90	<70	98	96[c]
HAB				
1. LiOH	180	<90	180	180
2. HC_2	180	<90	180	180[c]
3. HCO^+	180	<90	180	
4. HNN^+	180	<90	180	
5. HCO	135	<90	126	127[c]
6. HNN	180	<90	109	124[c]
7. HCN	180	<90	180	180
8. HNC	180	<90	180	180
9. HCF	95	95	108	101
10. HNO	115	<90	106	108
11. HO_2	110	<90	104	106
12. FOH	105	<90	99	97
AB_2				
1. C_3	180	<90	180	180
2. N_3^-	180	<90	180	180[d]
3. Li_2O	180	<90	180	180
4. CO_2	180	180	180	180
5. NO_2^+	180	180	180	180
6. NO_2	140	115	130	133
7. MgF_2	180	180	180	180
BAC				
1. LiCN	180	<90	180	180
2. LiNC	180	<90	180	180
3. FNO	115	115	112	110
AH_4				
1. BH_4^-	109	109	109	109[d]
2. CH_4	109	109	109	109
3. NH_4^+	109	109	109	109
A_2H_2				
1. C_2H_2 (cis)	180	180	180	180
2. C_2H_2 (trans)	180	150	180	180
3. N_2H_2 (cis)	115	<90	115	
4. N_2H_2 (trans)	110	<90	105	109[e]

[a] $<\theta$ means that up to θ, no minimum in E'_{VAL} is observed. [b] Reference 20. [c] Reference 19. [d] Reference 22. [e] Reference 21.

where P_{ab} is the density matrix element between atomic orbital a on atom A and b on atom B. The atomic orbitals are taken to be orthonormal. Presently, we use Löwdin orthogonalized basis functions.

Substituting for P_{ab} as

$$P_{ab} = \sum_{i} n_i c_{ia} c_{ib}$$

(11) Hehre, W. J.; Lathan, W. A.; Ditchfield, R.; Newton, M. D.; Pople, J. A. *Quantum Chemistry Program Exchange*, No. 236, University of Indiana, Bloomington.
(12) Armstrong, D. R.; Perkins, P. G.; Stewart, J. J. *J. Chem. Soc.* **1973**, 833, 2273.
(13) Semenov, S. G. *Theory of Valency in Progress*; Mir Publishers: Moscow, 1980; pp 150–169.
(14) Gopinathan, M. S.; Jug, K. *Theor. Chim. Acta* **1983**, *63*, 497.
(15) Buenker, R. J.; Peyerimhoff, S. D. *J. Chem. Phys.* **1966**, *45*, 3682. Peyerimhoff, S. D.; Buenker, R. J.; Whitten, J. L. *J. Chem. Phys.* **1967**, *46*, 1707. Pan, D. C.; Allen, L. C. *J. Chem. Phys.* **1967**, *46*, 1797. Rauk, A.; Allen, L. C.; Clementi, E. *J. Chem. Phys.* **1970**, *50*, 4133. Buenker, R. J.; Peyerimhoff, S. D. *Theor. Chim. Acta* **1972**, *24*, 132.
(16) Mulliken, R. S. *J. Am. Chem. Soc.* **1955**, *77*, 887.
(17) Gimarc, B. M. *J. Am. Chem. Soc.* **1971**, *93*, 815.

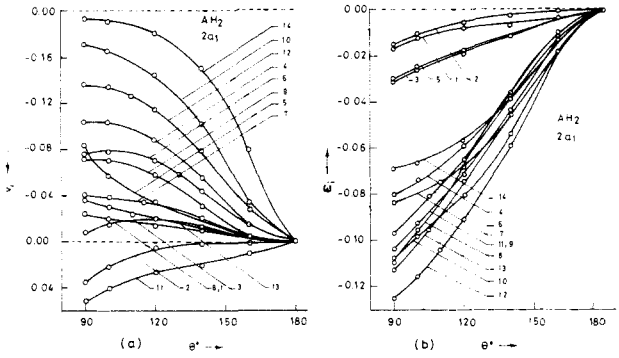

Figure 2. (a) MO valency variation of $2a_1$ of AH_2 molecules in the "reduced" form (see text). (b) MO eigenvalue variation of $2a_1$ of AH_2 molecules. For all figures in this article, curve numbers refer to molecule numbering in Table I.

and using eq 1 and 2, the molecular valency V_M can be expressed as a sum over occupied molecular orbitals

$$V_M = \sum_i v_i \tag{3}$$

with

$$v_i = \tfrac{1}{2}\sum_A^A \sum_a \sum_{B\neq A}^B \sum_b \sum_j n_i n_j c_{ia} c_{ib} c_{ja} c_{jb} \tag{4}$$

For open-shell systems, since in general $C_{ia}^{\alpha} \neq C_{ia}^{\beta}$, one should use the following generalization of eq 4.

$$v_i = \tfrac{1}{2}\sum_A^A \sum_a \sum_{B\neq A}^B \sum_b \sum_j [n_i^{\alpha} n_j^{\alpha} c_{ia}^{\alpha} c_{ib}^{\alpha} c_{ja}^{\alpha} c_{jb}^{\alpha} + n_i^{\alpha} n_j^{\beta} c_{ia}^{\alpha} c_{ib}^{\alpha} c_{ja}^{\beta} c_{jb}^{\beta} + n_i^{\beta} n_j^{\alpha} c_{ia}^{\beta} c_{ib}^{\beta} c_{ja}^{\alpha} c_{jb}^{\alpha} + n_i^{\beta} n_j^{\beta} c_{ia}^{\beta} c_{ib}^{\beta} c_{ja}^{\beta} c_{jb}^{\beta}] \tag{5}$$

MO valency, as defined above, is a measure of the probability of electron sharing between the atoms in that particular MO.[9] Thus for strongly bonding MOs, it has a value close to unity and for core, lone pair, and non- or anti-bonding orbitals, where the electron sharing is minimal, MO valency is very small. Plots of MO valency versus bond angle, which we shall call MO valency correlation diagrams, were given earlier[9] for H_2O, NH_3, HCN, HNC, LiOH, Li_2O, LiCN, and CO_2. These plots showed remarkable similarity to the original Walsh diagrams[1] for the corresponding class of compounds. In view of this, it is thought important to study the suitability of MO valency as the Walsh ordinate in the sense of satisfying criteria 1–3. We choose to study MO eigenvalue also from this point of view since many Walsh diagrams have appeared in the literature[3,4,15] with SCF MO eigenvalue as the ordinate.

All the MO valency and eigenvalue correlation curves displayed in this article have been shifted to a common origin, following Coulson and Deb's method of presentation,[8] by adding suitable constants since it is easier to visualize the slope of each curve in this "reduced" form than in conventional plots. These MO valency values will be referred to as reduced MO valencies. Note that as we have defined it (eq 5), v_i depends explicitly on orbital occupancy n_i, so that removal of an electron from a doubly occupied MO would reduce its valency by about half its original value. While this definition is convenient for the discussion of the bonding aspects of MOs, for checking criteria 1 and 2 it is desirable to scale the MO valencies of singly occupied MOs to that of double occupancy by multiplying by two. This has been done in Figures 2–6, 8–14, 16, 17, and 23.

We now discuss the salient features of the MO valency and eigenvalue correlation curves.

Figures 2a–4a give the MO valency correlation curves and Figures 2b–4b, 5, and 6 give the corresponding MO eigenvalue correlation curves for AH_2 systems. It is immediately clear from these figures that for AH_2 systems, the sign of the slope of a given MO is the same for most molecules, showing that both MO

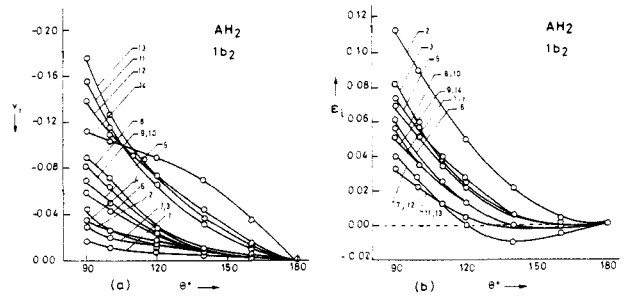

Figure 3. (a) MO valency variation of $1b_2$ of AH_2 molecules. (b) MO eigenvalue variation of $1b_2$ of AH_2 molecules.

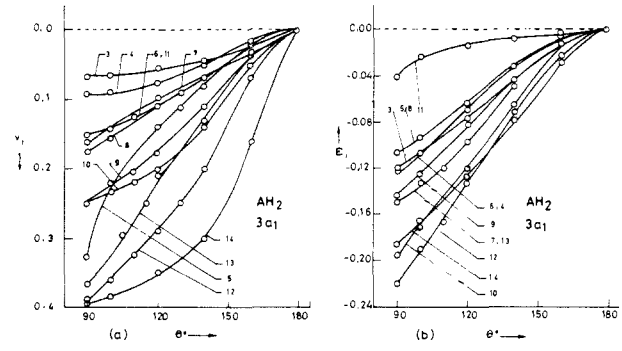

Figure 4. (a) MO valency variation of $3a_1$ of AH_2 molecules. (b) MO eigenvalue variation of $3a_1$ of AH_2 molecules.

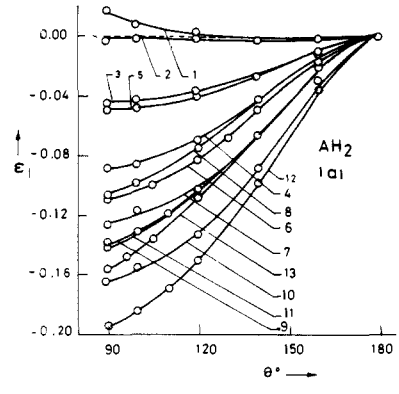

Figure 5. MO eigenvalue variation of $1a_1$ of AH_2 molecules.

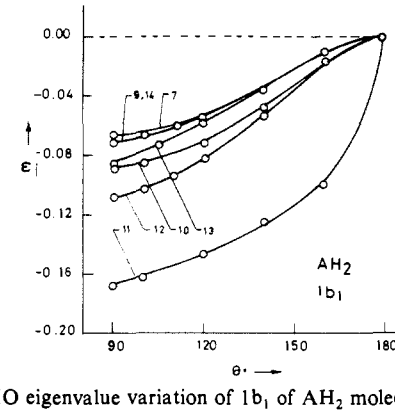

Figure 6. MO eigenvalue variation of $1b_1$ of AH_2 molecules.

valency and MO eigenvalue satisfy criterion 1. Similarly Figures 9–11 show that MO valencies of AH_3 systems also satisfy criterion 1. This is also true for MO eigenvalues of AH_3 systems, but the corresponding figures are not given here for reasons of space.

While the signs of the slopes of MO valency and MO eigenvalue correlation curves are generally the same, an exception occurs for the $2a_1$ MO (compare parts a and b of Figure 2). The $2a_1$ MO favors a linear geometry in the valency correlation diagram, as it does in the original Walsh diagram, whereas it favors a bent

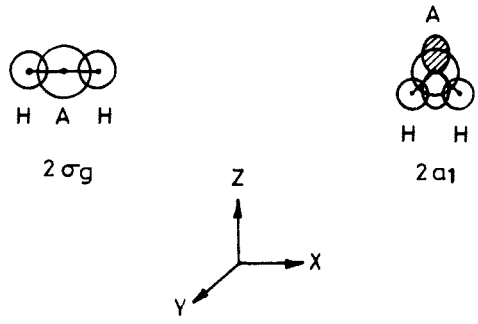

Figure 7. Composition of $2a_1$ MO of AH_2 at bent and linear geometries.

structure for the eigenvalue diagram. Walsh[1a] argued that $2a_1$ would favor a linear geometry because of the larger s orbital participation at 180° (Figure 7), whereas Mulliken[16] considered that the increased contribution of p_z at smaller angles would polarize the charge more effectively in the interatomic region and hence lower the energy of the $2a_1$ MO at bent geometries. An STO-3G overlap population analysis of the $2a_1$ MO of H_2S for example shows that while the s_H–p_{z_S} overlap population does increase from 90 to 180° by 0.046, the total atomic overlap population of the $2a_1$ MO is greater at 180° by 0.136. This may explain why $2a_1$ MO valency increases from bent to linear shape because MO valency also is a measure of the sharing of electrons between atoms. This explanation is further supported by the cases of BH_2^+ and H_2O^+, the two exceptions in Figure 2a, where the $2a_1$ overlap population decreases from 90 to 180°, thus showing that again overlap population and MO valency follow a similar trend.

To check if criterion 2 is satisfied by MO valency, it is only necessary to inspect whether the ratios v_i/v_j (where v_i and v_j are the reduced MO valencies for (i,j) pairs with opposite signs for the slopes) are uniformly less than unity or greater than unity. Presently, these ratios for the pairs $(2a_1,3a_1)$ and $(1b_2,3a_1)$ of AH_2 molecules and $(2a_1,3a_1)$ and $(1e,3a_1)$ of AH_3 molecules turn out to be uniformly less than one, indicating that $3a_1$ remains the dominating MO in all these compounds. The single exception occurs for the $(2a_1,3a_1)$ in BH_2^- for which the bond angle prediction by valency is also incorrect (see Section IV). The corresponding eigenvalue ratios ϵ_i/ϵ_j for the relevant pairs of orbitals are all again less than one. Thus criterion 2 is satisfied by both MO valency and MO eigenvalue.

Criterion 3 is strictly satisfied by MO valency since MO valencies for the core $1a_1$ of AH_2 and AH_3 molecules and the lone pair $1b_1$ of AH_2 molecules remain at zero for all bond angles. Hence no plots for these MOs are given here. However, criterion 3 does not hold good for MO eigenvalue since the eigenvalue plots of the core $1a_1$ of AH_2 (Figure 5) and the lone pair $1b_1$ (Figure 6) show a considerable variation with bond angle. The magnitude of their variation is comparable to that of a valence orbital, say $1b_2$ (Figure 3b).

To summarize our results so far, mo valency satisfies all the three criteria while the MO eigenvalue satisfies criteria 1 and 2 and not 3. With MO valency as the ordinate, we can therefore construct a universal correlation diagram for a given symmetry species. This is done by averaging the reduced valencies of each MO over all molecules of that symmetry species. The resulting universal valency correlation diagram for the AH_2 class is given in Figure 8a. This may be compared with the original Walsh diagram[1a] which is shown here in the "reduced" form (Figure 8b). These two diagrams are nearly identical. We have similarly constructed the universal eigenvalue correlation diagram (Figure 8c), which is seen to be quite different from the Walsh and valency diagrams.

The universal valency correlation diagram for the AH_3 species is displayed in Figure 12a. Comparison with the original Walsh[1d] diagram (Figure 12b) shows the remarkable similarity of the two diagrams. MO eigenvalues also lead to a similar universal diagram (Figure 12c) except for the core $1a_1$ curve which shows slight angle dependence.

For the other classes of compounds to be studied below, we restrict ourselves to the discussion of valency diagrams.

For all 12 HAB molecules studied here (see Table I), the valencies of 3a′, 4a′, 1a″, and 7a′ orbitals, with the single exception of 3a′ of LiOH, have the behaviour deduced by Walsh, namely that 3a′ and 4a′ favor linearity, 1a″ is more or less invariant to bond angle, and 7a′ strongly favors a bent shape. However, 5a′ and 6a′ merit special discussion.

Figures 13 and 14 give the valency plots for 5a′ and 6a′. Here we note that unlike all the other MOs discussed so far, these two MOs do not satisfy criterion 1. 5a′ favors a linear geometry for eight molecules while for the remaining four it favors a bent geometry. 6a′ indicates a bent structure for six molecules, and for five others it favors a linear shape. This behavior may be understood from Figure 15, which gives the qualitative energy correlation diagram for 5a′ and 6a′ of linear and bent molecules.[17] Though overlap considerations alone would predict that 5a′ favor linearity and 6a′ a bent shape, it is seen from Figure 15 that 5a′ and 6a′ become closer in energy on bending. If the 5σ and 1π are already close in energy, the two levels 5a′ and 6a′ can become nearly degenerate and will then diverge to avoid the forbidden crossing. This is shown by the broken lines in Figure 15. Hence for such molecules, 5a′ will favor a bent shape and 6a′ will favor linearity. This is why such behavior is observed for systems like HCO^+, HNN^+, HCN, and HNC (see Figures 13 and 14), where the energy separation ΔE between 5σ and 1π is much smaller than that for other systems (see Table II).

It can therefore be concluded that if an avoided crossing occurs for only some molecules of a given symmetry, no universal correlation diagram can be constructed. However, in such a case, a general valency correlation diagram can be drawn by showing the degenerate and nondegenerate situations separately. See, for example, the correlation curves for 5a′ and 6a′ orbitals of HAB in Figure 16a. Comparison of Figure 16a with the original HAB

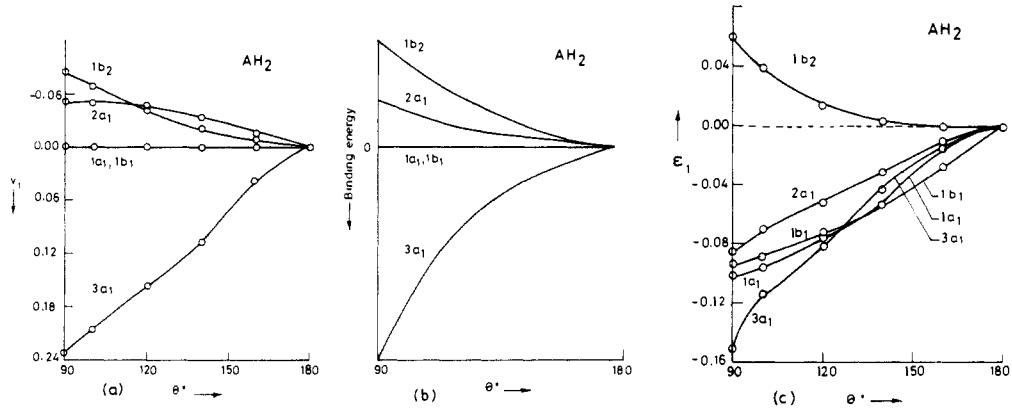

Figure 8. (a) Universal valency correlation diagram for AH_2. (b) AH_2 Walsh diagram in the "reduced" form, ref 1a. (c) Universal eigenvalue correlation diagram for AH_2.

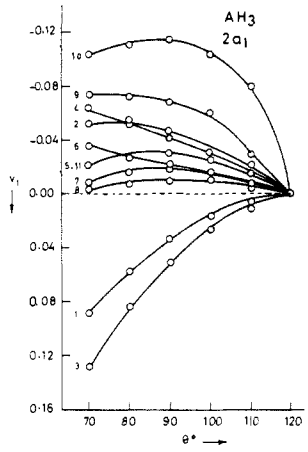

Figure 9. MO valency variation of $2a_1$ of AH_3 molecules.

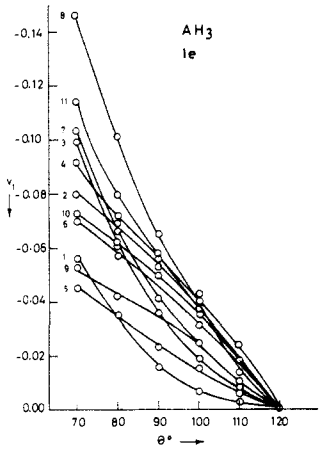

Figure 10. MO valency variation of 1e of AH_3 molecules.

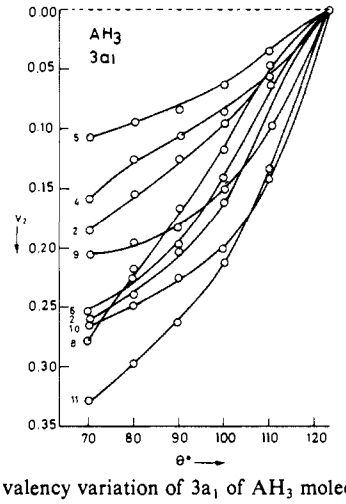

Figure 11. MO valency variation of $3a_1$ of AH_3 molecules.

correlation diagram given by Walsh[1c] (Figure 16b) shows a remarkable similarity, except for the behavior of the 5a′ and 6a′ orbitals.

The MO valency diagrams for the AB_2 molecules (not given here for want of space) generally satisfy criteria 1–3. Figure 17a gives the universal MO valency correlation diagram for the AB_2 molecules. This diagram is in agreement with Walsh's original diagram[1b] (Figure 17b), except for the $5a_1$ orbital, which shows a greater variation than that predicted by Walsh.

IV. Equilibrium Bond Angle and the Walsh Ordinate

Though the original Walsh diagrams were intended only for qualitative predictions of the shape of molecules, the question whether for an ordinate q_i, its sum over all occupied molecular orbitals, varies in the same way as the total energy E_T needs to be investigated if one is to extend the utility of correlation diagrams

Table II. Energy Separation between 5σ and 1π in Some HAB Molecules

molecule	ΔE (au)
Nearly Degenerate	
HCO^+	0.062
HNN^+	0.008
HCN	0.052
HNC	0.047
Nondegenerate	
HC_2	0.137
HCO	0.145
HNN	0.112

to the prediction of exact bond angle for various electronic states of a given molecule. For this purpose, we should examine if generally

$$\sum_i \partial q_i/\partial\theta \; (= \partial Q/\partial\theta) = \partial E_T/\partial\theta \tag{6}$$

or in particular

$$\sum_i \partial q_i/\partial\theta|_{\theta'} \; (= \partial Q/\partial\theta|_{\theta'}) = \partial E_T/\partial\theta|_{\theta'} \tag{7}$$

where θ' is the equilibrium bond angle.

With q_i as the ICSCF eigenvalue,[18] eq 6 holds exactly since the sum of the ICSCF eigenvalues is equal to the total SCF energy. For tempered orbital eigenvalues also, eq 6 holds for the few molecules studied.[7] In the case of canonical orbital eigenvalues it is well known[19] that their sum $\sum\epsilon_i$ $(=E')$ is not equal to the total molecular energy E_T. However, the relevant question is whether eq 6 and 7 hold with $Q = E'$. Though this was found to be true for some molecules,[4,15] a large number of exceptions were encountered.[8] In this section, we investigate whether with $Q = V_M$, where V_M is the molecular valency as defined by eq 3, eq 6 and 7 are satisfied.

Figures 18–22 give some typical results for the variation of V_M, E_T, and E' as a function of bond angle for some predominantly covalent compounds like H_2O, NH_3, and CO_2 as well as for the more ionic molecules like HCN and Li_2O. These figures also show the variation of E'_{VAL}, defined as the sum of eigenvalues of valence orbitals alone. For all these molecules $V_M(\theta)$ parallels $E_T(\theta)$, showing that eq 6 holds good for molecular valency. In sharp contrast to this, the bond angle dependence of E' and E'_{VAL} is often erroneous. See, for example, Figures 18, 19, 21, and 22. An example of a system where E' and E'_{VAL} show the correct behavior is CO_2 (Figure 20). It is also seen that E' and E'_{VAL} show virtually the same dependence on bond angle for all systems. This means that core orbital eigenvalues, even though they vary with bond angle, can be disregarded for bond angle predictions, as is usually done. It may be recalled that valency for core orbitals is invariant to bond angle and is almost zero so that $V_M = V_M^{VAL}$, and hence core orbitals do not affect predictions of bond angle by V_M.

To check the validity of eq 7, a detailed comparison of the equilibrium bond angles predicted by molecular valency, valence orbital eigenvalues, the STO-3G total energy, and the experimental values is made in Table I. For 50 of the 54 entries, V_M predicts the equilibrium bond angle within 10°, the average error in bond angle prediction being around 6°. Two molecules where V_M predictions are grossly in error are BH_2^- and HNN, which are wrongly predicted to be linear. Considering the eigenvalue predictions, we see from Table I that for as many as 32 of these 54 cases, the bond angle prediction is in serious error, no minimum in E'_{VAL} being found for many systems.

Hence we conclude that the $V_M(\theta)$ curve leads to reliable predictions of the ground-state bond angles whereas $E'(\theta)$ and

(18) Davidson, E. R. *J. Chem. Phys.* **1972**, *57*, 1999.
(19) Gimarc, B. M. *Molecular Structure and Bonding*; Academic: New York, 1979; pp 202–207.
(20) Mulliken, R. S.; Ermler, W. C. *Polyatomic Molecules*; Academic: New York, 1981.
(21) Baird, N. C.; Swenson, J. R. *Can. J. Chem.* **1973**, *51*, 3097.
(22) Radom, L. *Aust. J. Chem.* **1976**, *29*, 1635.

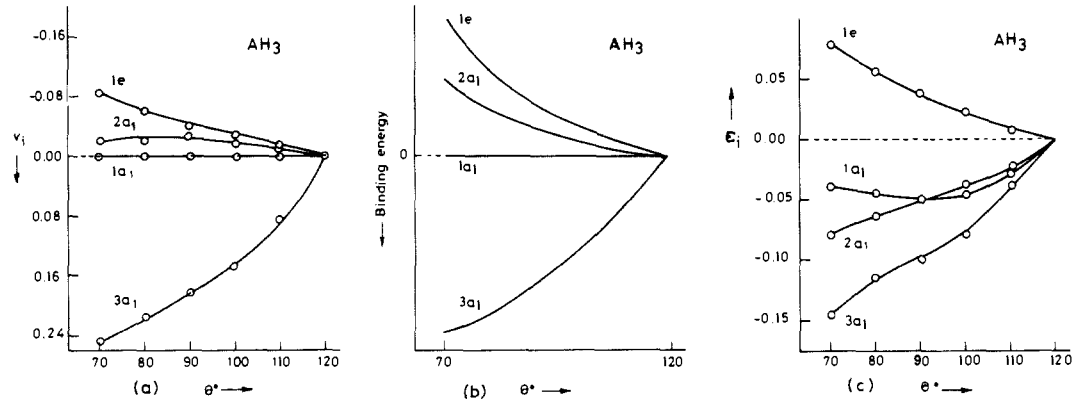

Figure 12. (a) Universal valency correlation diagram for AH_3. (b) AH_3 Walsh diagram, ref 1d. (c) Universal eigenvalue correlation diagram for AH_3.

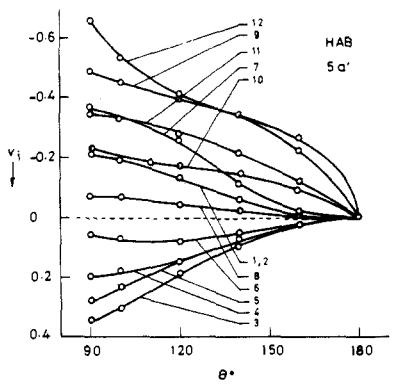

Figure 13. MO valency variation of 5a' of HAB molecules.

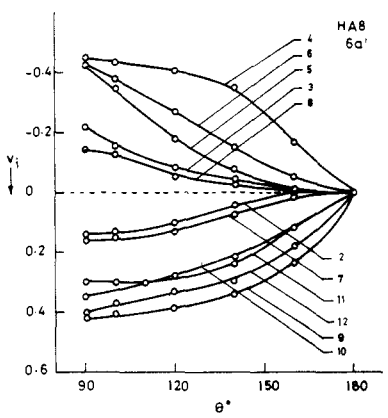

Figure 14. MO valency variation of 6a' of HAB molecules.

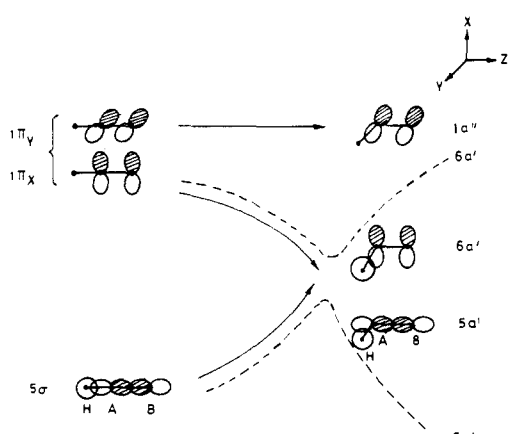

Figure 15. Schematic correlation diagram for 5σ (5a') and 1π (6a') of linear and bent HAB molecules. Broken lines indicate the divergence of 5a' and 6a' due to the non-crossing rule.

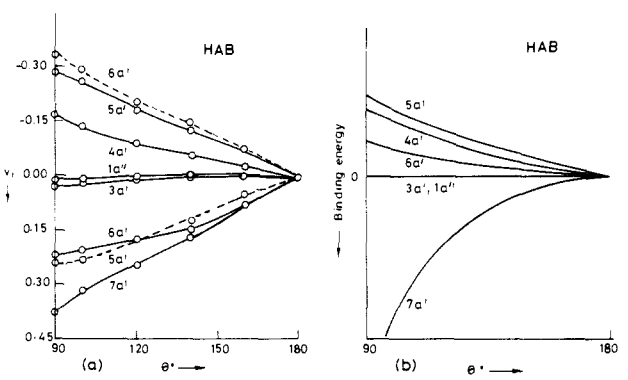

Figure 16. (a) General valency correlation diagram for HAB molecules. Broken lines indicate the correlations for nearly degenerate 5a' and 6a' orbitals (see text). (b) HAB Walsh diagram, ref 1c.

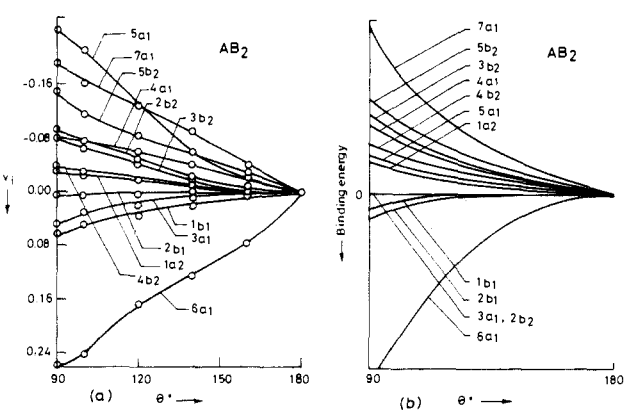

Figure 17. (a) Universal valency correlation diagram for AB_2 molecules. (b) AB_2 Walsh diagram, ref 1b.

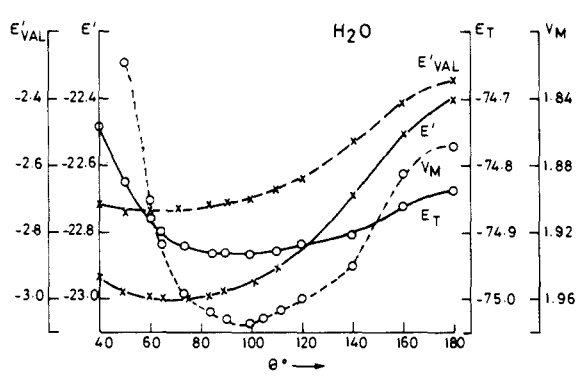

Figure 18. Variation of E'_{VAL}, E', V_M, and E_T with angle in H_2O. Energies in au.

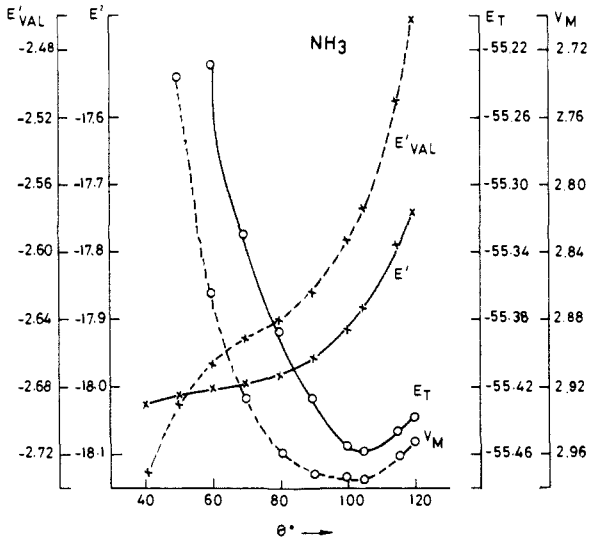

Figure 19. Variation of E'_{VAL}, E', V_M, and E_T with angle in NH_3. Energies in au.

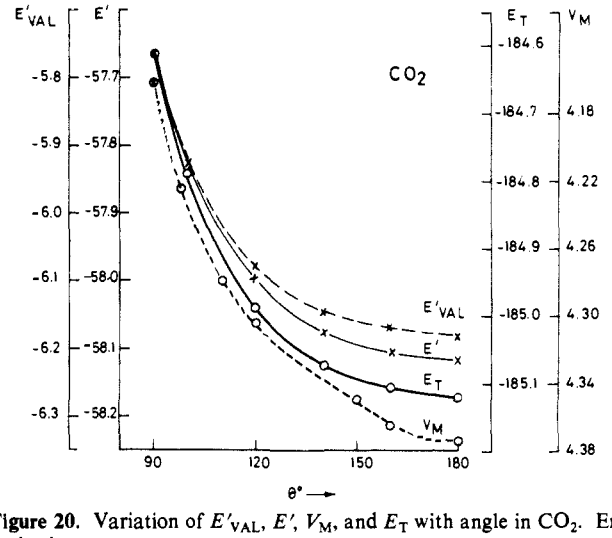

Figure 20. Variation of E'_{VAL}, E', V_M, and E_T with angle in CO_2. Energies in au.

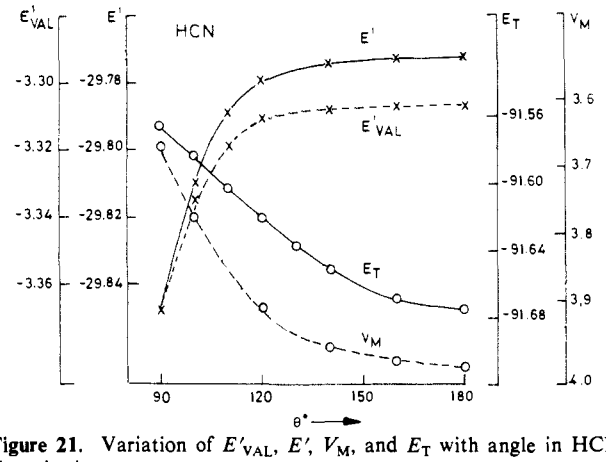

Figure 21. Variation of E'_{VAL}, E', V_M, and E_T with angle in HCN. Energies in au.

$E'_{VAL}(\theta)$ curves are unsatisfactory in this respect.

V. A Simple Valency Method for Excited States

In the previous section, we confined our attention to the bond angles of molecules in their ground state and found that molecular valency V_M provides a very reliable prediction of the ground-state bond angles. It would be interesting to see if equilibrium bond angles of excited states also can be similarly predicted, since ab initio calculations are laborious for such states due to the necessity for the inclusion of configuration interaction (CI).[23]

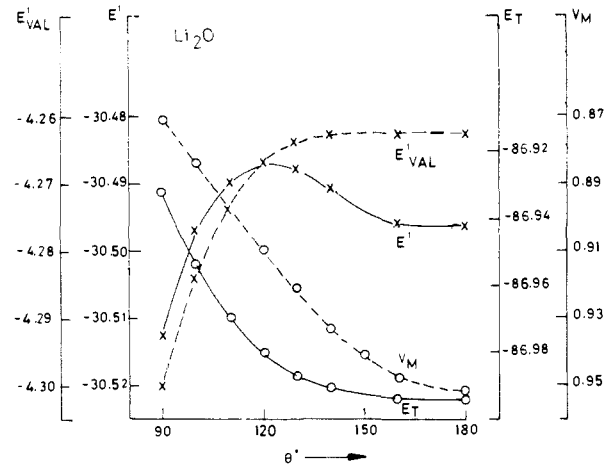

Figure 22. Variation in E'_{VAL}, E', V_M, and E_T with angle in Li_2O. Energies in au.

To construct a MO valency correlation diagram and from that to calculate the $V_M(\theta)$ curve, one has to do a full SCF calculation at various angles. The fact that a $V_M(\theta)$ versus θ curve gives nearly the exact equilibrium bond angle for the ground state, as demonstrated above, may be of theoretical interest but not of much practical value since an SCF calculation has anyway got to be performed at each angle. It is desirable to avoid such calculations for the excited states, and hence in this section, we present a simple procedure for the construction of a $V_M(\theta)$ curve for various excited or ionized states of molecules using only the wave function of the ground state.

The procedure that we propose to construct MO correlation diagrams for different electronic states of a molecule is as follows:

(a) A ground-state SCF calculation of the molecule at various bond angles is performed.

(b) Excited or ionized electronic configurations of the molecule are obtained simply by feeding electrons in the occupied and virtual orbitals of the ground state from (a) as required.

(c) Molecular orbital valency at a particular bond angle is now calculated by using eq 5 with the MO occupancies and coefficients as in (b).

As a typical example of a system exhibiting widely different bond angles for its various electronic states, MO valency correlation diagrams for the ground state of H_2O and the $^2B_1$, $^2A_1$, and $^2B_2$ states of H_2O^+, constructed according to the above procedure, are displayed in Figure 23a–d. Inspection of thse diagrams shows that the general criteria 1–3 for a Walsh ordinate are satisfied for these ionized states also. [Notice that $3a_1$ and $1b_2$ orbitals in $^2A_1$ and $^2B_2$ states of H_2O^+ respectively (Figure 23, parts c and d) are singly occupied and hence their valencies must be multiplied by two when comparing with doubly occupied $3a_1$ and $1b_2$ curves in the other diagrams. However, calculation of the molecular valency V_M should obviously be done with use of the actual MO valency values given in these figures.]

It is straightforward now to obtain the $V_M(\theta)$ versus θ curves for these states by simply summing up the valencies for the appropriate occupied orbitals, as given by eq 3. We have presently plotted $\Delta V(\theta)$, the difference of the molecular valency at a particular bond angle from the maximum value, i.e., $V_M(\theta) - V_M^{MAX}$ versus θ. These curves are shown in Figure 24. The equilibrium bond angles obtained by CI calculation[24] are also indicated in this

(23) Hostany, R. P.; Dunning, T. H., Jr.; Gilman, R. R.; Pipano, A.; Shavitt, I. *J. Chem. Phys.* **1975**, *62*, 4764.
(24) Meyer, W. *Int. J. Quantum Chem. Symp.* **1971**, *5*, 341.
(25) Demoulin, D.; Jungen, M. *Theor. Chim. Acta* **1974**, *34*, 1. Demoulin, D. *Chem. Phys.* **1975**, *11*, 329.
(26) Schwenzer, G. M.; O'Neil, S. V.; Schaefer, H. F., III; Baskin, C. P.; Bender, C. F. *J. Chem. Phys.* **1974**, *60*, 2787.
(27) Chu, S. Y.; Goodman, L. *J. Am. Chem. Soc.* **1975**, *97*, 7.

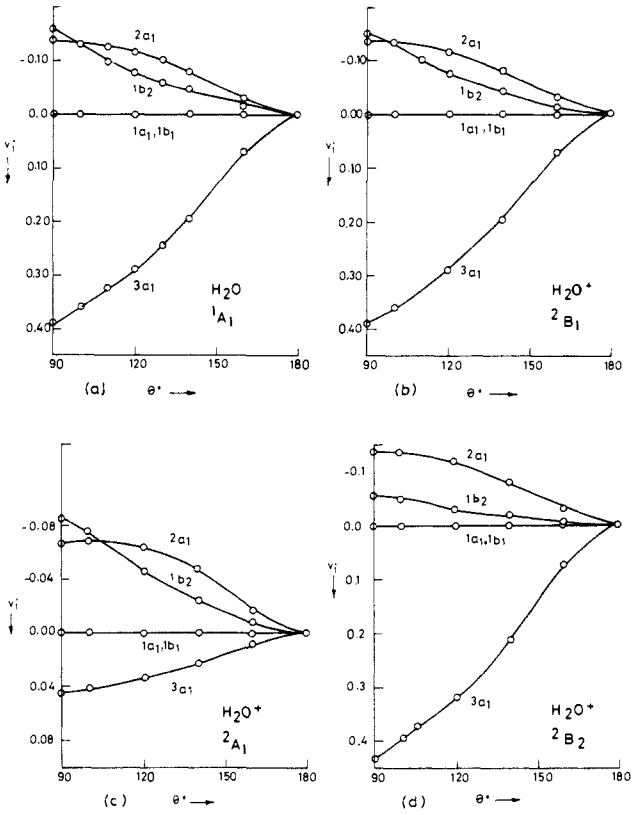

Figure 23. MO valency correlation diagram for (a) the ground state of H_2O, (b) the $^2B_1$ state of H_2O^+, (c) the $^2A_1$ state of H_2O^+, and (d) the $^2B_2$ state of H_2O^+.

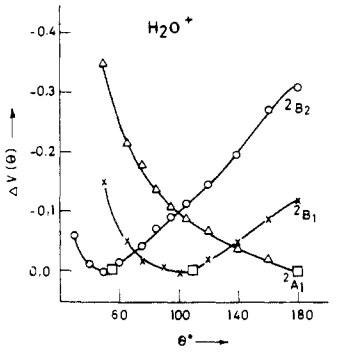

Figure 24. Plots of $\Delta V(\theta)$ versus θ for $^2B_1$, $^2A_1$, and $^2B_2$ states of H_2O^+. An open square denotes the equilibrium bond angle calculated with CI (see Table III).

figure. It is gratifying to note the excellent agreement obtained by our present valency prediction and the reported CI values. What is remarkable is that even a very acute angle of 55° for the $^2B_2$ state of H_2O^+ is reproduced well by the present method which gives 50°.

We have applied the present valency method for the prediction of excited and ionized state bond angles to a variety of systems. The results are in surprisingly good agreement with the available CI values (see Table III). The table also includes results for some states for which CI calculations have not been reported so far. The present valency method thus affords a simple and economical way of predicting the equilibrium bond angle of any electronically excited state of a molecule merely from the knowledge of its ground-state wave function.

Another interesting feature of the present method is that one can also obtain the valencies of atoms in the excited states of molecules. Atomic valency has been shown to be of value in the prediction of reactivities of atoms,[28] molecular strain,[29] as well as the radical nature of molecules.[30] One can obtain the density matrix element P_{ab} for the excited state using the ground-state molecular orbitals (occupied and virtual) as in step (b) above. Use of this P_{ab} in eq 1 will then give the atomic valency in the excited state. The accuracy of this method may be seen from the comparison of atomic valency values in HCN^- as an example. The

Table III. Valency Prediction of Bond Angles of Excited and Ionized States of Molecules

molecule	outer electronic configuration	state	bond angle present	bond angle ab initio[a]
BH_2^+	$(1b_2)^2$	$^1A_1$	180	180
BH_2	$(3a_1)^0(1b_1)^1$	$^2B_1$	180	180
	$(1b_2)^1(3a_1)^2$	$^2B_2$	55	
	$(1b_2)^1(3a_1)^1(1b_1)^1$	$^4A_2$	55	
	$(2a_1)^1(1b_2)^2(3a_1)^2$	$^2A_1$	108	
	$(2a_1)^1(1b_2)^2(3a_1)^1(1b_1)^1$	$^4B_1$	180	
BH_2^-	$(3a_1)^1(1b_1)^1$	$^3B_1$	135	136, 140
	$(3a_1)^0(1b_1)^2$	$^1A_1$	180	180
CH_2	$(3a_1)^2$	$^1A_1$	100	101
	$(1b_2)^1(3a_1)^2(1b_1)^1$	$^3A_2$	52	
	$(1b_2)^1(3a_1)^1(1b_1)^2$	$^3B_1$	48	
	$(2a_1)^1(1b_2)^2(3a_1)^2(1b_1)^1$	$^3B_1$	95	
	$(2a_1)^1(1b_2)^2(3a_1)^1(1b_1)^2$	$^3A_1$	180	
CH_2^-	$(3a_1)^1(1b_1)^2$	$^2A_1$	100	104
NH_2^+	$(3a_1)^1(1b_1)^1$	$^3B_1$	138	140
	$(3a_1)^1(1b_1)^1$	$^1B_1$	180	180
	$(3a_1)^0(1b_1)^2$	$^1A_1$	180	180
NH_2	$(3a_1)^1(1b_1)^2$	$^2A_1$	138	143
	$(1b_2)^1(3a_1)^2(1b_1)^2$	$^2B_2$	55	48
	$(2a_1)^1(1b_2)^2(3a_1)^2(1b_1)^2$	$^2A_1$	97	
NH_2^-	$(3a_1)^2(1b_1)^2$	$^1A_1$	100	103
H_2O^+	$(3a_1)^2(1b_1)^1$	$^2B_1$	100	111
	$(3a_1)^1(1b_1)^2$	$^2A_1$	180	180
	$(1b_2)^1(3a_1)^2(1b_1)^2$	$^2B_2$	50	55
	$(2a_1)^1(1b_2)^2(3a_1)^2(1b_1)^2$	$^2A_1$	90	
HCN	$(1a'')^1(7a')^1$	$^3A''$	115	123
	$(1a'')^1(2a'')^1$	$^3A'$	155	160[b]
	$(5a')^1(6a')^2(1a'')^2(7a')^1$	$^3A'$	135	
	$(5a')^1(6a')^2(1a'')^2(2a'')^1$	$^3A''$	180	
	$(1a'')^1(8a')^1$	$^3A''$	180	
	$(5a')^1(6a')^2(1a'')^2(8a')^1$	$^3A'$	180	
HCN^-	$(1a'')^2(7a')^1$	$^2A'$	145	140
HNC	$(1a'')^1(7a')^1$	$^3A''$	124	113
	$(6a')^1(1a'')^2(2a'')^1$	$^3A''$	154	157
HNC^-	$(1a'')^2(7a')^1$	$^2A'$	135	140
CO_2^+	$(1a_2)^2(4b_2)^1$	$^2B_2$	180	180
CO_2	$(4b_2)^1(6a_1)^1$	$^3B_2$	165	140
	$(4b_2)^1(2b_1)^1$	$^3A_2$	180	180
CO_2^-	$(4b_2)^2(6a_1)^1$	$^2A_1$	163	135
	$(4b_2)^2(2b_1)^1$	$^2B_1$	180	180
NO_2^+	$(4b_2)^2$	$^1A_1$	180	180
NO_2	$(4b_2)^1(6a_1)^2$	$^2B_2$	115	104
	$(1a_2)^1(4b_2)^2(6a_1)^2$	$^2A_2$	115	102
	$(4b_2)^2(2b_1)^1$	$^2B_1$	180	180
	$(1a_2)^1(4b_2)^2(6a_1)^1(2b_1)^1$	$^2B_2$	140	122
	$(4b_2)^2(7a_1)^1$	$^2A_1$	180	180
NO_2^-	$(4b_2)^2(6a_1)^2$	$^1A_1$	124	118
NO_2^{2-}	$(4b_2)^2(6a_1)^2(2b_1)^1$	$^2B_1$	122	
$C_2H_2^+$	$(3b_u)^1(1a_u)^2$	^2B_u	180	180
	$(1a_u)^1$	^2A_u	180	180
C_2H_2	$(1a_u)^1(4a_g)^1$	^3A_u	165	170[c], 121
	$(3b_u)^1(1a_u)^2(4a_g)^1$	^3B_u	170	170[c], 131
	$(3b_u)^1(1a_u)^2(1b_g)^1$	^2A_u	180	
$C_2H_2^-$	$(4a_g)^1$	^2A_g	162	113[d]
	$(1b_g)^1$	^2B_g	180	

[a] Reference 20. [b] Reference 26. [c] HCH angle found by holding C_2H_2 planar; ref 25. The same procedure adopted presently. [d] Reference 27.

(28) Gopinathan, M. S.; Jug, K. *Theor. Chim. Acta* **1983**, *63*, 511.
(29) Siddarth, P.; Gopinathan, M. S. *J. Mol. Struct.* **1986**, *148*, 101.
(30) Jug, K.; Gopinathan, M. S. *Theor. Chim. Acta* **1985**, *68*, 343.

Table IV. Atomic Valency Values Obtained with the Present Method for Different States of HCN[a]

molecule	state	V_C	V_N	V_H
HCN	$^1A'$	(3.98)	(3.01)	(0.99)
HCN	$^3A''$	3.04	2.12	0.96
HCN^-	$^2A''$	3.28	2.37	0.90
		(3.23)	(2.33)	(0.96)

[a] Values in parentheses are the actual atomic valencies obtained with the STO-3G wave function.

atomic valency values for HCN^- calculated by the present procedure (using the wave function for HCN) and that obtained from the SCF wave function for HCN^- are in good agreement (see Table IV). Hence one may use the present simple procedure to obtain atomic valencies in various electronic states.

The effect of electronic excitation on atomic valencies may be illustrated by considering HCN. According to the valency prediction, $1a'' \rightarrow 7a'$ excitation (i.e., $^1A'$ state to $^3A''$ state) leads to a significant bending of the molecule (see Table III). There is considerable reduction in the valencies of C and N (Table IV) and consequent weakening of the C–N bond. In HCN^-, with a bond angle of 145°, valencies of C and N are again reduced, though not to the same extent as in the $^3A''$ state of HCN. It would be interesting to apply the present method to study the changes in atomic and interatomic valency on molecular excitation and ionization and correlate them with reactivity, strain, and the radical nature of excited species.

VI. Conclusions

The general criteria for a molecular orbital quantity to serve as a successful Walsh ordinate in the sense of giving correct qualitative predictions of molecular shape are formulated as follows. The sign and relative magnitude of the slopes of a given MO should remain the same for different molecules of a particular symmetry species and the core and lone pair orbitals should not be affected by bond angle variation. We have studied how well the two ordinates, the recently proposed MO valency and the commonly used MO eigenvalue, satisfy these criteria. It is found that both of these ordinates are suitable for the generation of universal correlation diagrams, which are in reasonable agreement with the original Walsh diagrams. It is, however, noted that core and lone pair orbital eigenvalues vary considerably with bond angle, in contrast to the original Walsh diagrams and the present valency correlation diagrams.

The fact that MO valency and MO eigenvalue correlation diagrams are similar does not imply that both would lead to the same quantitative bond angle predictions. It is the actual magnitudes of the slopes that are important for predicting the correct bond angle. The sum of eigenvalues often leads to serious errors in bond angle predictions, its plot as a function of bond angle exhibiting no minimum in several cases. In contrast, molecular valency, defined as the sum of molecular orbital valencies, predicts the ground-state bond angles to a fair degree of accuracy.

This finding is relevant when applied to the prediction of bond angles of excited states of molecules, which are not easily calculated otherwise. In this paper, we have proposed a simple valency method to determine equilibrium bond angles of any electronically excited, ionized, or reduced state of a molecule purely from its ground-state wave function. It is seen that this method gives results that are in good agreement with values obtained from CI calculations. Further, valencies of atoms in excited states of molecules can also be determined with this method. These atomic valencies might be of use in predicting the reactivity, strain, and radical nature of molecules in the excited states.

Band Electronic Structure Study of the Semimetallic Properties and the Anisotropic Resistivity Hump in $ZrTe_3$

Enric Canadell,*[1a] Yves Mathey,[1b] and Myung-Hwan Whangbo*[1c]

Contribution from the Laboratoire de Chimie Théorique and Laboratoire de Spectrochimie des Eléments de Transition, Université de Paris-Sud, 91405 Orsay, France, and the Department of Chemistry, North Carolina State University, Raleigh, North Carolina 27695-8204.
Received June 1, 1987

Abstract: Tight-binding band calculations were carried out on $ZrTe_3$ to examine its semimetallic properties and anisotropic resistivity hump at ~63 K. Our calculations show that adoption of the type B structure is crucial for the semimetallic nature of $ZrTe_3$. The overlapping of the Te 5p-block bands with the Zr 4d-block bands gives rise to a pair of nested electron pockets and a pair of nested hole pockets, all of which have the shape of a flat cylinder whose axis is perpendicular to the chain direction. Thus, a charge density wave formation associated with the Fermi surface nesting does not affect the electrical conductivity of $ZrTe_3$ along the chain direction, so that the resistivity hump is observed only along the directions perpendicular to the chain axis.

Transition-metal trichalcogenides MX_3 (M = Ti, Zr, Hf; X = S, Se, Te)[2] consist of layers of composition MX_3. Each MX_3 layer is made up of trigonal-prismatic MX_3 chains, in which each X_3 triangle has a shape with one side much shorter than the other two. This leads to the oxidation formalism $(X^{2-})(X_2^{2-})$ for X_3[3] so that the formal oxidation state of the metal is M^{4+} (d^0), and thus the metal d-block bands of MX_3 are expected to be empty. In agreement with this prediction, all MX_3 compounds except for $ZrTe_3$ are found to be semiconductors with band gaps ranging from ~1 to ≳2 eV.[2b,4] If the electronic structure of $ZrTe_3$ is

(1) (a) Laboratoire de Chimie Théorique, Université de Paris-Sud. (b) Laboratoire de Spectrochimie des Elements de Transition, Université de Paris-Sud. Present address: Département de Physique, Faculté de Sciences de Luminy, 13288 Marseille. (c) Department of Chemistry, North Carolina State University.

(2) (a) Meerschaut, A.; Rouxel, J. *Crystal Structures and Properties of Materials with Quasi-One-Dimensional Structures*; Rouxel, J., Ed.; Reidel: Dordrecht, The Netherlands, 1986; p 222. (b) Bullett, D. W. *Theoretical Aspects of Band Structures and Electronic Properties of Pseudo-One-Dimensional Solids*; Kamimura, H., Ed.; Reidel: Dordrecht, The Netherlands, 1985, p 163. (c) Hulliger, F. *Structural Chemistry of Layer-Type Phases*; Lévy, F., Ed.; Reidel: Dordrecht, The Netherlands, 1976; p 247.

(3) Whangbo, M.-H. *Crystal Structures and Properties of Materials with Quasi-One-Dimensional Structures*; Rouxel, J. Ed.; Reidel: Dordrecht, The Netherlands, 1986; p 27.

(4) (a) Brattas, L.; Kjekshus, A. *Acta Chem. Scand.* **1972**, *26*, 3441. (b) Kurita, S.; Straehli, J. L.; Guzzi, M.; Lévy, F. *Physica* **1981**, *105B*, 169. (c) Herr, S. L.; Brill, J. W. *Synth. Metals* **1986**, *16*, 283. (d) Khumalo, F. S.; Olson, C. G.; Lynch, D. W. *Physica* **1981**, *105B*, 163. (e) Grimmeiss, H. G.; Rabenau, A.; Hahn, H.; Neiss, P. *Z. Elektrochem.* **1961**, *65*, 776. (f) Schairer, W.; Shafer, M. W. *Phys. Status Solidi.* **1973**, *A17*, 181. (g) Khumalo, F. S.; Hughes, H. P. *Phys. Rev.* **1980**, *B4*, 2078. (h) Perluzzo, G.; Jandl, S.; Girard, P. E. *Can. J. Phys.* **1980**, *58*, 143. (i) Nee, S. F.; Nee, T. W.; Fan, S. F.; Lynch, D. W. *Phys. Status Solidi.* **1982**, *B113*, K5.

0002-7863/88/1510-0104$01.50/0